Science of the Total Environment 958 (2025) 178040

Contents lists available at ScienceDirect

Science of the Total Environment

journal homepage: www.elsevier.com/locate/scitotenv

Molecular shifts in dissolved organic matter along a burn severity continuum for common land cover types in the Pacific Northwest, USA

J. Alan Roebuck Jr [a], Samantha Grieger [a], Morgan E. Barnes [a], Xia Gillespie [a], Kevin D. Bladon [b], John D. Bailey [b], Emily B. Graham [a,c], Rosalie Chu [d], William Kew [d], Timothy D. Scheibe [e], Allison N. Myers-Pigg [a,f,*]

[a] Biological Sciences Division, Pacific Northwest National Laboratory, Sequim, WA, USA
[b] College of Forestry, Oregon State University, Corvallis, OR, USA
[c] School of Biological Sciences, Washington State University, Pullman, WA, USA
[d] Environmental Molecular Sciences Laboratory, Pacific Northwest National Laboratory, Richland, WA, USA
[e] Pacific Northwest National Laboratory, Richland, WA, USA
[f] Department of Environmental Sciences, College of Natural Sciences & Mathematics, University of Toledo, Toledo, OH, USA

HIGHLIGHTS

- Land cover type, rather than burn severity, was a key driver of DOC leachability from burned chars.
- Burn severity was a key driver of DOM composition leached from vegetation of different land cover types.
- DOM's unique molecular composition from different land cover types converged as burn severity increased.

GRAPHICAL ABSTRACT

ARTICLE INFO

Editor: Roland Bol

ABSTRACT

Increasing wildfire severity is of growing concern in the western United States, with consequences for the production, composition, and mobilization of dissolved organic matter (DOM) from terrestrial to aquatic systems. Our current understanding of wildfire impacted DOM (often termed pyrogenic DOM) composition is largely built from temperature-based studies that can be difficult to extrapolate to field conditions, which are often defined by 'burn severity', or the post-wildfire impact observed at a site. Thus, burn severity can encapsulate a broader range of fire and environmental conditions not exclusive to temperature. Biogeochemical studies that describe DOM along burn severity continuums remain limited but are needed to better link DOM composition with field conditions post-fire. In this study, we addressed this need with an experimental open air burn simulation that generated chars from vegetation representative of major land cover types in the western United States. The chars were leached to simulate DOM mobilization potential. The DOM composition was characterized by ultra-high resolution mass spectrometry (HR-MS) and UV/VIS absorbance and fluorescence. Our results indicated that the shifts of DOM production and composition along a burn-severity gradient depends on the land cover type that

* Corresponding author at: Biological Sciences Division, Pacific Northwest National Laboratory, Sequim, WA, USA.
E-mail address: allison.myers-pigg@pnnl.gov (A.N. Myers-Pigg).

https://doi.org/10.1016/j.scitotenv.2024.178040
Received 2 August 2024; Received in revised form 11 November 2024; Accepted 8 December 2024
Available online 14 December 2024

was burned, with the degree of change dependent on the composition of the starting parent vegetation material. Fluorescence signatures indicated a strong convergence across land cover types to more aromatic DOM with increasing severity, while HR-MS indicated an increase in the production of aromatic nitrogen containing DOM with increasing severity. Results from this study enhance our ability to describe DOM composition in a framework that can be more directly related with field and remote-sensing based metrics.

1. Introduction

Wildfires have historically been a natural disturbance agent for ecosystems in the Pacific Northwest (PNW), USA; however, climate change has increased the area burned and frequency of large wildfires in the region since the mid-twentieth century (Littell et al., 2010). While the annual area burned has not been outside of historical fire regimes at millennial-scales (Marlon et al., 2012; Reilly et al., 2017), the recent increases have been linked with climatic factors that have also contributed to increases in burn severity for many areas of the PNW (Francis et al., 2023; Halofsky et al., 2020; Reilly et al., 2017). In the PNW, fires span a range of major ecoregions that vary in land cover characteristics and in historical fire frequency, intensity, and severity. At the broadest level, these ecoregions can be binned into four land cover types based on the major vegetation type present (Supplemental information). These four bins of land cover types represent the bulk of fire activity in the region since the mid-1980s (Fig. 1A). Forested regions (e.g., Douglas-fir and mixed conifer forest), in particular, are areas where the majority of high severity fire activity has occurred (Reilly et al., 2017) and has seen major increases since 2017 due to an uptick in megafires with burn areas >40,000 ha (Fig. 1B). Comparatively, there has also been a rise in area burned in shrubland dominant land cover, including mountain woodlands that represent transitional areas between mountainous forest and valley shrubland regions (Fig. 1B). In contrast to forested regions, shrubland dominant regions are typically fuel limited, decreasing the risk of high severity impacts (Stavi, 2019).

An increase in wildfire burn severity has considerable implications for watersheds (Bowman et al., 2009) including the restructuring of surface soils and incomplete combustion of soil organic matter into pyrogenic organic matter (PyOM) (Santín et al., 2015). This has potential to significantly alter terrestrial carbon balances by shifting the carbon carrying capacity of terrestrial ecosystems and reallocation of carbon from above to below ground (Bodí et al., 2014; Boot et al., 2014; Hudiburg et al., 2023). Global estimates of annual PyOM production currently stand around 373 TgC per year, with up to 212 Pg stored in soils (Santín et al., 2016). Not all PyOM remains local as a significant

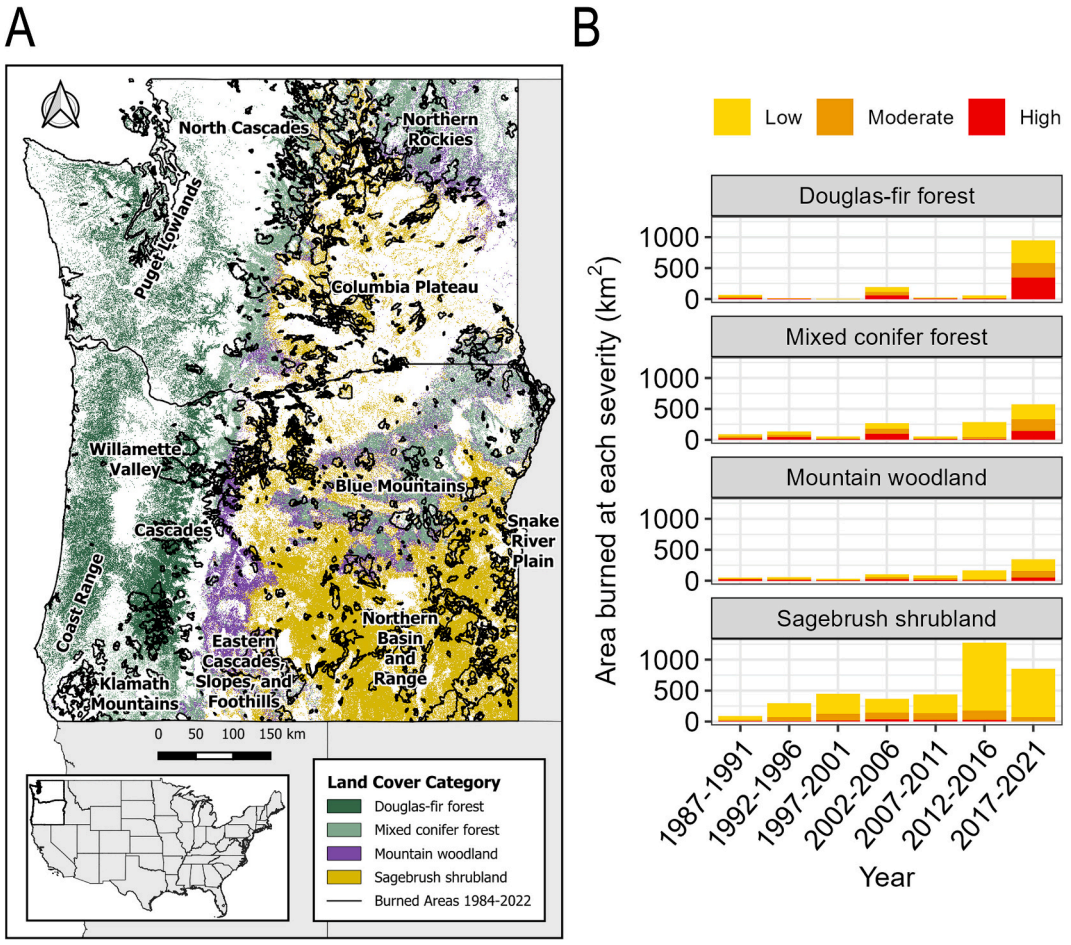

Fig. 1. A) Map of Pacific Northwest (PNW) states Washington and Oregon highlighting key land cover classes across the PNW and burn areas (black boundaries) from the years 1984–2022. Burned area obtained from Monitoring Trends in Burn Severity (MTBS) data layers (https://mtbs.gov). Note that samples collected in this study are representative of these major land cover classes and this map does not show geographic area of where experimental samples were collected.
B) Area burned at various burn severities for 4 major land cover classifications in the Pacific Northwest (Washington and Oregon) in 5-year intervals. Data obtained from the Monitoring Trends in Burn Severity database (https://mtbs.gov).

fraction can be mobilized to aquatic systems during major precipitation events in the form dissolved organic matter (DOM) (often termed as pyrogenic DOM) (Myers-Pigg et al., 2017; Roebuck et al., 2018a, 2022), where as much as 10 % (27 Tg) of the DOM exported from rivers to coastal waterways globally is of pyrogenic origin (Coppola and Druffel, 2016; Jaffé et al., 2013). There is further evidence that shifts in major land cover types can impact the chemical composition of fire impacted DOM transported in aquatic systems (Roebuck Jr et al., 2018b; Serafim et al., 2023; Wagner et al., 2015b); however, such linkages across burn severities within major PNW land cover types remain unexplored.

Understanding shifts in DOM and nutrient delivery to aquatic systems post-fire is important for managing water resources (Bladon et al., 2014) and impacts on downstream aquatic ecosystem processes (Dahm et al., 2015; Rust et al., 2019). Wildfire impacted DOM, for instance, has shown enhanced disinfection bioproduct formation potential, relevant for post-fire water treatment (Cawley et al., 2017; H. Chen et al., 2022; Zhao Li et al., 2023). Additionally, wildfire impacted DOM can impact biofilm enzyme activities, metal binding and transport, sediment stoichiometry, and aquatic photochemical processes, which can all alter in-stream microbial dynamics and aquatic nutrient cycles (Bostick et al., 2020; Y. Chen et al., 2022; Shakesby et al., 2015; Thuile Bistarelli et al., 2021). Such processes drive the ultimate fate of wildfire impacted DOM. For instance, increased N uptake into the DOM pool post-fire can increase bioavailability (de la Rosa and Knicker, 2011), potentially limiting its transport through soils and aquatic systems. Alternatively, highly aromatic DOM produced during wildfires may have minimal reactivity and can be exported more rapidly to coastal systems (Coppola et al., 2022). Despite the importance of DOM on aquatic biogeochemistry, its chemical make-up in relation to fire impacts is not well parameterized for developing predictive understandings of changing fire severity on aquatic ecosystem functions.

Current literature on wildfire impacted DOM has placed great emphasis on temperature-based proxies for understanding production, reactivity, and fate (Masiello, 2004; Wagner et al., 2018). Chemical markers that include low temperature combustion products like anhydrosugars or higher temperature polycondensed aromatic compounds have been regularly used as wildfire signatures in aquatic systems (Wagner et al., 2018). While there is inherent value to such proxies, linking such knowledge with field-based observations is challenging as data on soil and ground temperatures during wildfires are often unavailable and field conditions result in more heterogeneous burning conditions than laboratory counterparts (Brucker et al., 2022). Currently, assessments of wildfire impact on the landscape, such as those from the US Forest Services Burned Area Emergency Response (BAER), rely more heavily on the metric of 'burn severity' for ground-truthing post-fire impacts. In such assessments, burn severity is characterized based on visual cues of post-fire forest floor dynamics (e.g., organic matter losses), physical damages, and ash deposition (Keeley, 2009). As such, burn severity may not always be linear with temperature as it encapsulates a range of local factors including burn duration, quality of fuel (e.g., vegetation), and moisture conditions (Keeley, 2009). Studies have recently begun to recognize the importance of post-fire visual indicators of burn severity in biogeochemical studies (Vega et al., 2013), resulting in an increase in the use of this metric in watershed-scale biogeochemical models to describe fire impacts on aquatic ecosystems (Zhi Li et al., 2023; Wampler et al., 2023). Surprisingly, though, there are no studies to our knowledge that contextualize DOM production and shifting composition in this framework, which limits the extrapolation of relevant information to field conditions and utilization in biogeochemical models.

Further complicating our understanding of fire impacted DOM cycling in aquatic systems is that knowledge of chemical transformations is fragmented due to analytical limitations available for characterization (Zimmerman and Mitra, 2017). While chemical markers have been routinely used to identify and quantify fire impacted DOM exports (Dittmar et al., 2012; Myers-Pigg et al., 2017; Roebuck Jr et al., 2018a), it remains unfeasible to target every individual component of the pyrogenic spectrum. Recent studies have begun to recognize the utility of other non-targeted bulk scale analyses to provide insights into the chemical behavior of fire impacted DOM from soils, chars, and in natural waters (Roebuck et al., 2022; Wozniak et al., 2020; Zhang et al., 2023; Zhu et al., 2024). Ultra-high resolution mass spectrometry, for example, has provided novel information on the speciation and cycling of dissolved pyrogenic nitrogen (Roth et al., 2022; Wagner et al., 2015a; Wozniak et al., 2020). Excitation-emission fluorescence has been further used to understand optical characteristics of temperature treated soils, biochars, and post-fire soil DOM (Cawley et al., 2017; Li et al., 2017; McKay et al., 2020; Rajapaksha et al., 2019; Yin et al., 2024) and is increasingly used to monitor post-fire water quality in aquatic systems (Johnston and Maher, 2022; Olivares et al., 2019). Collectively, there remains underexplored potential for use of these techniques in tandem to describe wildfire related transformations of DOM in aquatic systems in a framing that can be better linked with field-based observations (though see Cao et al. (2024) and Yin et al. (2024) who utilize these combined approaches to better understand soil DOM post-fire).

In our study, we used open air burn experiments to provide a comprehensive overview of DOM production and composition from leached chars created along a burn severity continuum. The chars represented vegetation from the major land cover types described in Fig. 1. Ultra-high resolution mass spectrometry and excitation-emission matrices were used to describe the composition of leached DOM. Within that context, we asked the following questions:

(1) Does the amount of DOM available for mobilization from charred materials shift based on land cover type and/or burn severity?
(2) How does the composition of DOM evolve along a burn severity continuum and what impact does land cover type play in this evolution?

We first hypothesized that the amount of DOM leached would be highest in low severity chars, as low temperature chars have been observed to release highly soluble organic carbon (Luo et al., 2011; Norwood et al., 2013). We hypothesized that the DOM composition would shift systematically with increasing burn severity to include more aromatic and nitrogen rich signatures, analogous to observations along heat temperature treatments (Wozniak et al., 2020). However, different vegetation types are well known to produce variable DOM signatures (Hansen et al., 2016), and recent studies have indicated that different vegetation charred under similar conditions yield variable DOM signals (Wozniak et al., 2020). Thus, we hypothesized the extent to which DOM transformations would occur with increased burn severity would be indicative of the land cover types in our study.

2. Methods

2.1. Vegetation collection and open air burn experiments

The overarching experimental design followed four major steps detailed below and in Section 2.2 (Fig. S1). First, vegetation was collected from common fire-prone landscapes in watersheds within the Pacific Northwest (Grieger et al., 2022). These archetypal land cover types included Douglas-fir forests (*Pseudotsuga menziesii*), mixed conifer forests (*Pseudotsuga menziesii* and *Pinus ponderosa*), mountain woodland (*Pinus ponderosa* and *Artemisia tridentata*) and sagebrush shrubland (*Artemisia tridentata*). Unless otherwise specified in the text, we broadly group the land cover types as forest dominant (Douglas-fir forest, mixed conifer forest) or shrubland dominant (mountain woodland, sagebrush shrubland). We have provided more details on land cover types in the Supporting information.

Second, chars were generated from these plant materials using an open air burn table to represent a range of environmental variability and burn conditions by manipulating common burn parameters including

temperature, duration of heating, moisture conditions, and plant senescence (e.g., living or dead). For all samples, the ratio of woody to canopy materials by mass was held constant at 40 % canopy materials (<0.5 cm) and 60 % woody (>0.5 cm) material. The burn simulations were performed with each vegetation sample using an open air burn table configured at a 5° angle with metal barriers to separate vegetation treatments (Grieger et al., 2022). Straw was used as an initial fire starter in the bottom most quadrant of the table, and the metal barriers were opened only briefly to allow flames to enter subsequent quadrants and more rapidly start the combustion process. We placed two thermocouples (Omega Ceramic Fiber Thermocouple Elements, insulation temperature rating up to 1200 °C), wired to a datalogger (Campbell Scientific CR1000) in each quadrant (six thermocouples total) to quantify temperature and duration for each burn. Grab samples of charred and burned materials were taken twice as temperatures reached roughly 300 °C and 600 °C using sanitized tongs and placed in sanitized metal trays.

Once temperatures cooled, any remaining char and completely combusted ash material were also collected (Step 3 in Fig. S1). Burn severity was assigned to each char based on visual cues derived from field-based assessments that include ash color, degree of charring, and degree of consumption (Parsons et al., 2010). Chars were dried and stored in a well-ventilated dark area at room temperature until further analysis. A more comprehensive assessment for this open air burn experiment, including information on vegetation collection and treatments, burn protocols, burn table details, as well as workflows, photos, and videos, is available on the Environmental System Science Data Infrastructure for a Virtual Ecosystem (ESS-DIVE) data repository (Grieger et al., 2022).

2.2. Leaching experiments

Triplicate leachates were generated for each land cover type for both unburned and each char grab sample by shaking 25 g of unground material with 1 L of synthetic rainwater in furnaced Pyrex glass bottles at 160 rpm in the dark at 25 °C for 24 h (Step 4, Fig. S1). Synthetic rainwater was prepared with an ionic strength characteristic to that of the PNW, excluding ions containing carbon or nitrogen (see Grieger et al. (2022) for complete preparation protocols that are outlined in the "BSLE_Laboratory_Protocol" file located within the Methods folder). Leachates were strained through a 2 mm × 0.6 mm opening PTFE mesh followed by vacuum filtration through furnaced 0.7 μm GF/F filters and a subsequent 0.2 μm Gamma irradiated filter. Aliquots were taken for subsequent analysis detailed below and stored at 4 °C until the analysis was performed.

2.3. Leachate chemistry

2.3.1. Total and dissolved organic carbon

Total carbon (TC) was measured on finely ground unburned and charred material using an elemental analyzer (ECS 8020; NC Technologies, Italy). Dissolved organic carbon (DOC) was measured on the leachates with a Shimadzu TOC-L Total Organic Carbon Analyzer. The DOC was measured as non-purgeable organic carbon through online acidification with phosphoric acid and purging to remove inorganic carbon. Mobilization of DOC was defined as the DOC leached normalized to the TC in the unburned or charred material, giving units of mg DOC/g TC.

2.3.2. UV-VIS absorbance and fluorescence

Absorbance and fluorescence measurements were measured simultaneously with a Horiba Aqualog. Absorbance scans were recorded at a wavelength range from 230 to 800 nm in 3 nm intervals. Fluorescence was measured as 3D excitation-emission matrices (EEM) with the same wavelength parameters. All EEMs were post-processed in Matlab 2020b that included blank subtraction, inner filter correction (Ohno, 2002), and Raman normalization from daily water Raman scans collected at an excitation of 350 nm. All EEMs were further subjected to parallel factor analysis (PARAFAC) using the drEEM toolbox v. 6.0 for Matlab (https://openfluor.org) (Murphy et al., 2013). A 6-component model was split-validated with non-negativity constraints and explained 99.3 % of the variability across the dataset.

2.3.3. Fourier transform ion cyclotron resonance mass spectrometry

High resolution mass spectra were collected via Fourier transform ion cyclotron resonance mass spectrometry for individual samples at the Environmental Molecular Sciences Laboratory in Richland, WA with a 21 T in house built spectrometer (Shaw et al., 2016). Methanol extracts from SPE were injected into the electrospray ionization (ESI) source at a DOC concentration of 50 mg/L. Four hundred fifty micro scans were averaged in negative mode at a mass range of m/z 200 to 900 with internal calibrations applied. Chemical formulae of C, H, O, N, S, and P were assigned to peaks with S/N > 2 and mass measurement error < 0.5 ppm using Formularity (Tolić et al., 2017). Peaks were further assigned based on their elemental formula into common biomolecular groups as described by (Seidel et al., 2015). Assignments to these groups do not indicate positive identification of individual formulae, but rather stoichiometric similarity to the associated biomolecule(s). Further processing to calculate common molecular indices including the modified aromaticity index (AI_{mod}), double bond equivalents, and nominal oxidation state of carbon (NOSC) (Koch and Dittmar, 2006, 2016; LaRowe and Van Cappellen, 2011) were calculated with the 'fticrrr' package for R (Patel, 2020). Intensity weighted averages were calculated for individual elements (C, H, O, N, and S) and molecular properties for each sample.

2.4. Statistical approaches

All statistical analysis and figures were generated with the R programming language version 4.3.1 (R Core Team, 2023) with all codes available to reproduce findings available at Myers-Pigg et al. (2024b). For all hypothesis testing, model assumptions of normality were assessed with Shapiro-Wilk test. Levene's test was further used to confirm assumptions of equal variance. In cases where this assumption was violated, a heteroskedasticity correction was applied (White, 1980). For all tests, significance was determined at an alpha level of 0.05 where significance was considered "weak" when $0.01 < p < 0.05$ and "strong" when $p < 0.01$.

For leachate samples, linear mixed effects (LME) models were performed with the lme4 package (Bates et al., 2015) to test the importance of fixed effects (burn severity, land cover type) and their interaction on DOC concentrations. Triplicate replication within the experimental design was accounted for as the random effect. Analysis of variance (ANOVA) were used to test the significance of the interaction term within the LME models. When the interaction term was not significant, LME models were re-run removing the interaction term and significance between the primary fixed effects was determined. Post hoc pairwise comparisons based on Tukey's Honest Significant Difference were conducted with the emmeans package (Lenth, 2023).

Finally, principal components analysis (PCA) was performed based on the relative distribution of PARAFAC components to identify trends in fluorescence signatures across land cover types and burn conditions.

3. Results

3.1. Char burn severities

The range of experimental burning conditions generated chars from across a range of burn temperatures and burn durations, resulting in chars that span low to high burn severities (Table S1). It should be noted that we were unable to obtain burn conditions that would generate high severity chars for the sagebrush shrubland land cover type.

3.2. Dissolved organic carbon and absorbance characterization of char leachates

The DOC leached from the unburned plant materials and burned chars across land cover types is presented normalized to total particulate carbon in Fig. 2a. Across the whole dataset, leached DOC ranged from 3.7 to 121.4 mg DOC/g TC. The amount leached was notably higher for the sagebrush shrubland (33 to 121 mg DOC/g TC) and mountain woodland (17 to 72 mg DOC/g TC) compared to the Douglas-fir forest (4 to 47 mg DOC/g TC) and mixed conifer forest (4 to 68 mg DOC/g TC). Land cover type was the primary driver influencing the amount of DOC leached ($p < 0.001$, df = 3, $F = 16.0425$), whereas burn severity was not significant ($p > 0.05$, df = 3, $F = 2.0539$) based on two-way LME models (Table S2).

In contrast to DOC, LME models provided support that $SUVA_{254}$ was more directly linked with burn severity ($p < 0.001$, df = 3, $F = 22.7756$; Table S3). In particular, $SUVA_{254}$ increased consistently from <1.5 L/mgC·m in the unburned leachates up to ~2.5 L/mgC·m in the moderate to high severity leachates, indicating a shift to more aromatic DOM leached with increasing burn severity. It is important to note that while $SUVA_{254}$ was directly linked with burn severity, direct correlations with maximum charring temperature were not significant for three of the four land cover types (mixed conifer forest: $r = 0.29$; mountain woodland: $r = 0.34$; sagebrush shrubland: $r = 0.55$; all $p > 0.05$) and was weakly significant for the Douglas-fir forest ($r = 0.61$, $p = 0.02$).

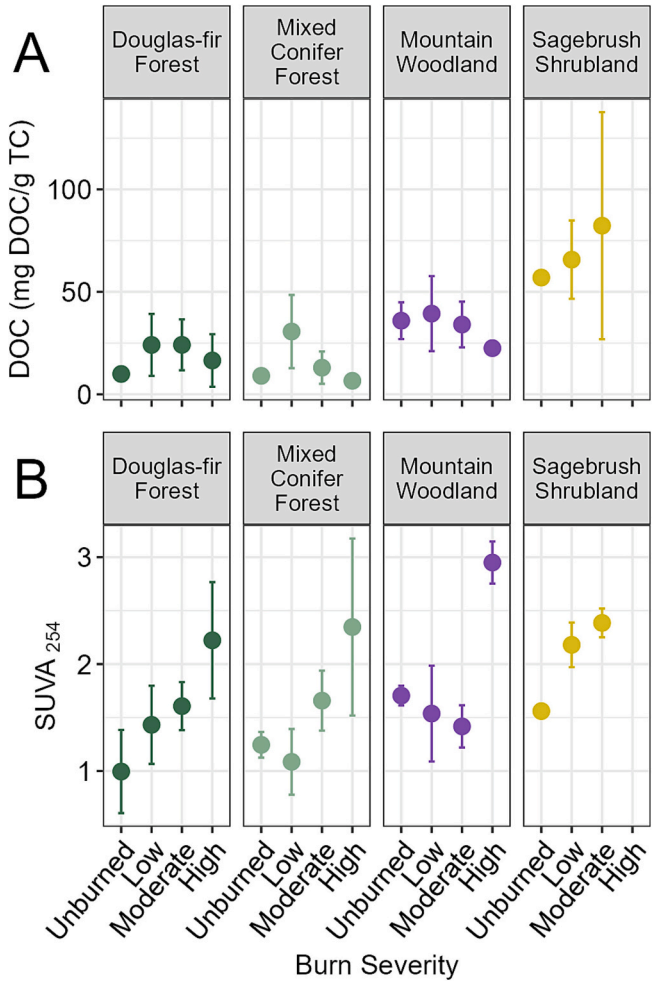

Fig. 2. A) Normalized DOC to total carbon in unburned or charred solid material and B) $SUVA_{254}$ for unburned and char leachates for each land cover type. Note that high severity burn conditions were unachievable for the sagebrush shrubland (Methods Section 2.1).

3.3. Fluorescence characterization of char leachates

Leachates from the unburned and burned land cover types yielded a 6 component PARAFAC model derived from excitation-emission matrices with a range of identified fluorophores characteristic of natural organic matter in aquatic systems (Table S4) (Coble, 1996; Stedmon et al., 2003; Wünsch et al., 2019). Leachates in the unburned forested land cover types (including both Douglas-fir forest and mixed conifer forest) were enriched with the low emission wavelength protein-like component C1, with relative proportions typically >60 % (Table 1; Fig. S1). In contrast, unburned shrubland land cover types were enriched with component C5 (>40 % in mountain woodland, >30 % in sagebrush shrubland, Table 1; Fig. S1). This component represents long wavelength emission and has an emission maximum roughly 35 nm greater than that of the common microbial humic-like M peak (Table S4). This component remains unclassified and would be considered unique if observed in natural waters (Wünsch et al., 2019). A cross-reference within the OpenFluor database (www.openfluor.org) provided only two matches with other studies for which this component has been observed, with the most relevant identifying this component in leaf leachates of tulip trees (Wheeler et al., 2017). The presence of this component across various vegetation types with limited presence in aquatic systems indicates this signal may be a leaching specific signature that becomes either integrated or lost when incorporated into the broader DOM pool.

As vegetation burns at higher severities, fluorescence signatures in leachates from forested land cover types shift from low wavelength emission protein-like components C1 in favor of components that had higher emission wavelengths relative to C1 (e.g., red-shifting). For example, component C2, which represents the commonly identified peak A (UV humic-like), and C3, which represents peak M (microbial humic-like), were each elevated in high severity forest leachates (Table 1; Fig. S1). For shrubland land cover types, blue-shifting (higher to lower emission maximums) was observed as the proportion of high emission wavelength C5 was depleted, also in favor of increasing C2 and C3 that were lower in emission maximums relative to C5 (Fig. S1, Table S4). These shifts across land cover types led to a convergence among PARAFAC signatures, which is best exemplified through principal component analysis (Fig. 3). In the PCA, burn severity was the primary driver along PC1 (53.3 %) and land cover type was the primary driver along PC2 (22 %). PC2 separates the forest and shrubland land cover types by the protein-like C1 and high emission wavelength C5, respectively. With increasing burn severity, samples converged positively along PC1 indicating a systematic shift of leachate DOM from the unburned parent signatures to more enriched components C2 and C3. As such, DOM composition in the forest land cover types represented a shift from predominantly protein-like signatures to higher emission wavelength signals. Comparatively, the shrubland vegetation leachates represented a shift from higher to lower emission wavelength signals (Figs. 3; S1).

3.4. Molecular characterization of char leachates with FTICR-MS

High resolution mass spectrometry characterization of unburned and char leachates revealed trends across the burn continuum that were specific to land cover type. The bulk of FTICR-MS signal in the leachates were primarily from highly unsaturated compounds in both forest (~45 %) and shrubland (~60 %) land cover types (Fig. 4). More nuanced differences were observed among the land cover types for compounds with elevated H/C ratios (>1.5). For instance, in the unburned forested samples, aliphatic and aliphatic-N containing compounds (e.g., peptide-like) represented about 30 % of the spectral signal (Fig. 4). With increasing burn severity, this peptide-like signal decreased in favor of more condensed aromatic compounds ($AI_{mod} > 0.67$), which contributed up to 50 % of the total signal in the high severity leachates (Fig. 4). This shift was further complemented with a shift toward an overall

Table 1
Table of mean and standard deviation of PARAFAC components across burn severity gradient and land cover type.

Land cover type	Burn severity	C1%	C2%	C3%	C4%	C5%	C6%
Douglas-fir forest	Unburned	74.1 ± 2.4	9.6 ± 3.0	2.6 ± 0.1	3.4 ± 2.4	2.9 ± 0.6	7.4 ± 3.4
	Low severity	51.1 ± 8.6	13.2 ± 4.5	8.7 ± 1.3	6.6 ± 2.2	3.2 ± 0.7	17.2 ± 3.4
	Moderate severity	37.3 ± 6.1	24.0 ± 7.4	11.4 ± 0.8	9.0 ± 0.7	2.2 ± 0.9	15.7 ± 1.7
	High severity	10.0 ± 13.6	48.0 ± 11.2	19.5 ± 5.7	10.6 ± 1.4	2.3 ± 1.9	9.6 ± 3.8
Mixed conifer forest	Unburned	71.6 ± 2.0	7.4 ± 1.2	2.8 ± 0.7	3.2 ± 1.1	2.5 ± 0.5	12.5 ± 4.2
	Low severity	68.9 ± 7.7	7.9 ± 3.1	5.5 ± 2.0	2.8 ± 2.2	2.9 ± 0.7	12.0 ± 3.2
	Moderate severity	21.2 ± 19.3	37.2 ± 18.6	17.7 ± 6.5	9.2 ± 1.3	3.1 ± 1.9	11.6 ± 4.9
	High severity	0.7 ± 1.1	56.7 ± 2.7	26.0 ± 5.0	8.2 ± 3.3	2.7 ± 2.4	5.6 ± 6.2
Mountain woodland	Unburned	29.5 ± 4.2	6.5 ± 1.0	0.9 ± 1.1	2.8 ± 2.7	49.4 ± 10.3	10.9 ± 1.3
	Low severity	42.7 ± 12.1	9.2 ± 2.5	7.9 ± 1.9	7.5 ± 4.0	18.4 ± 7.4	14.4 ± 1.9
	Moderate severity	47.0 ± 23.0	18.7 ± 13.4	9.8 ± 4.5	8.3 ± 5.8	4.9 ± 2.4	11.2 ± 2.4
	High severity	0.5 ± 0.6	46.0 ± 4.5	25.9 ± 1.0	16.9 ± 4.0	0.0 ± 0.1	10.7 ± 1.3
Sagebrush shrubland	Unburned	30.7	7.0	3.2	10.2	34.5	14.3
	Low severity	13.7 ± 2.6	14.4 ± 3.7	12.9 ± 1.6	26.7 ± 7.8	18.8 ± 8.8	13.4 ± 1.7
	Moderate severity	2.9 ± 0.4	33.1 ± 2.4	25.6 ± 0.7	23.5 ± 1.5	1.5 ± 0.6	13.4 ± 1.4

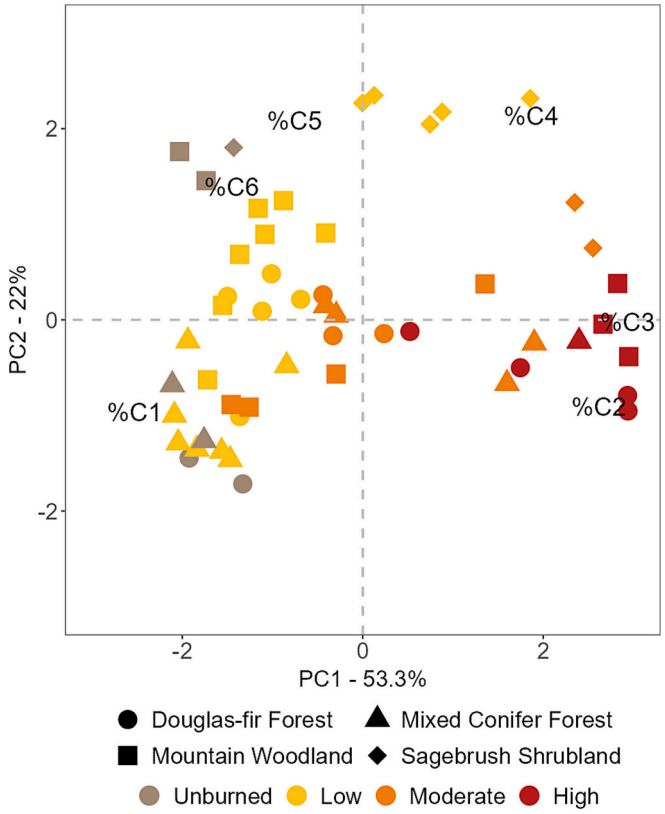

Fig. 3. Principal Component Analysis (PCA) highlighting multivariate shifts in EEM-PARAFAC components from each land cover type across the burn severity continuum.

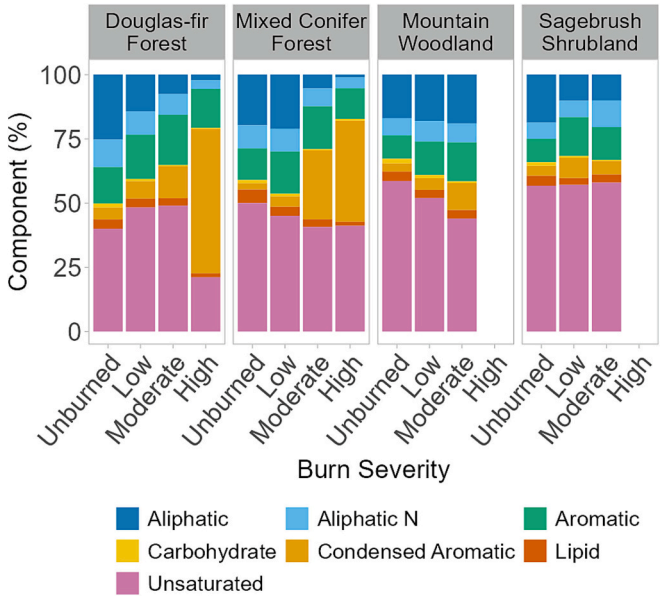

Fig. 4. Relative proportion of signal from inferred biochemical classes derived from FTICR-MS for all land cover types across the burn severity continuum. Note that groupings do not constitute positive identification, but rather an acknowledgement of stoichiometric similarities.

higher aromaticity index from 0.1 to 0.6 and an increase in the intensity weighted N signal from 0.6 to 1.1, indicating production of more complex N containing aromatic signals (Figs. 4, S2).

In contrast to the forest leachates, the molecular response of shrubland leachate DOM to burning was more muted. For instance, there was no change in the signal represented by condensed aromatic compounds (Fig. 4). Instead, there was an observed change in measured signal of aromatic compounds ($0.67 > AI_{mod} > 0.5$) from 5 % in the unburned leachates up to 15 % from the moderate severity burn leachates (Fig. 4). Additionally, the intensity weighted N signature increased in the sagebrush shrubland from 0.6 in the unburned leachates to 1.2 in the moderate severity leachates. This N increase appeared to be, in part, linked with an increase in protein-like formula, which increased from 6.6 % in the unburned leachate to 10.4 % in the moderate severity leachate (Fig. 4).

4. Discussion

4.1. Land cover type is a key indicator of post-fire DOC leachability across a burn severity continuum

The leachability of DOC from charred materials was more dependent on the land cover type rather than burn severity. The higher leachability of DOC from sagebrush shrubland chars may be attributed to compositional differences in the parent material, which has been previously reported in a comparison of oak and grassland chars (Bostick et al., 2018; Mukherjee and Zimmerman, 2013; Wozniak et al., 2020). Shrubland species typically contain lower percentages of insoluble lignin-like moieties compared to woody forested vegetation (Cook and Harris, 1968; Fengel and Wegener, 2011; Kufeld et al., 1981; Rahman et al., 2013; Welch, 1997), which may have led to the higher leachability of DOC from shrubland chars in this study. This is supported in the high resolution molecular data where sagebrush shrubland was composed of more unsaturated, lignin-like degradation products compared to the

forest vegetation (Fig. 4). Similarly, the proportion of highly condensed aromatic compounds produced across the burn severity continuum was considerably lower than that of the forest land cover types (Fig. 4) again indicating a potentially more favorable solubility of the shrubland land cover types. It is notable that the mountain woodland, which represents a mix of ponderosa pine and sagebrush shrubland vegetation, conformed primarily to sagebrush shrubland molecular signatures (Fig. 4). As such, the mountain woodland land cover types, which spatially represent a transitional zone between mountainous forest and valley shrublands in the western United States, conformed to an intermediate DOC leachability between the forested land cover types and the sagebrush shrubland. Collectively, these results implicate land cover type as a key component that should be considered in biogeochemical frameworks that seek to understand mobilization of DOC in fire impacted aquatic systems. Furthermore, such results may have implications for linking post-wildfire shifts in carbon directly with remote sensing products, which may help fill a gap in both conceptual and earth system models.

While land cover type was the key driver of DOC mobilization from fire impacted chars, burn severity was notably not significant in explaining DOC leached in the burned chars (Fig. 1). This result was surprising and led to a rejection of our hypothesis that chars created at low burn severities would result in greater leaching of DOC as described by other studies along burn temperature gradients (Bostick et al., 2018; Cawley et al., 2017; Liu et al., 2015; Mukherjee and Zimmerman, 2013; Wilkerson and Rosario-Ortiz, 2021; Zhang et al., 2023). For instance, Zhang et al. (2023) reported temperature thresholds for forest soils at 225 °C, peaking at around 12 % of the total organic carbon leached as DOC. This is comparable with our study, where we observed the amount of DOC leached ranged from 3.7 to 121.4 mg DOC/g TC (0.37 to 12.1 % TC as DOC) across all land cover types and burn severities. While similar in magnitude, the disconnect between overall trends across the burn continuum observed in our study relative to those in other studies may be attributable to differences in experimental design. This is best exemplified in a recent study that highlighted major differences in leachability for chars generated in open air burning compared with temperature-based muffle furnaces that are more commonly used in other studies (Myers-Pigg et al., 2024a). In particular, our open air study was designed to encompass a range of burn conditions (e.g., temperature, duration of heating) and environmental variability (e.g., vegetation type, living vs dead vegetation, dry vs wet; see methods Section 2.1) that may be broadly expected in a naturally burned system. Such wide-ranging variability at the ecosystem level may mute temperature-explicit DOC signals that are often reported in other studies, highlighting the need to better integrate field-based measurements of fire impact (e.g. burn severity) and land cover type when considering post-fire impacts on DOC export to aquatic systems.

We recognize a slight limitation in our sampling design driven by the inability to achieve burn conditions that would create high severity chars with the sagebrush shrubland vegetation. While this is also typical of field-based observations where high severity burns are less probable in sagebrush dominant ecosystems (Stavi, 2019) (Fig. 1a), we were unable to directly assess the interactive role of high severity burns on DOC leached across the different land cover types due to its absence in the study for the sagebrush shrubland. However, we recognize empirically in the forest land cover types that decreasing trends in high severity leachates exists (Fig. 2a). We further note comparable observations within the compositional data where >50 % of the molecular level signatures in the forest leachates were composed of condensed aromatic compounds (Fig. 4) and optical signatures that broadly implicate an increased aromatic signature (Figs. 2b, 3). Condensed aromatic compounds typically make up the residual chemical make-up of high temperature charcoals and ash (Bird et al., 2015). Such compounds are notably less soluble than non-fire impacted particulate organic matter, however, they can make up a disproportionate contribution of the DOM signatures derived from these burned sources (Bostick et al., 2018; Zhang et al., 2023). Thus, while we cannot directly assess its statistical significance, our empirical observations are consistent with the paradigm that chars generated at high burn severity will generate a less soluble, but more aromatic DOM pool.

4.2. DOM composition from different land cover types becomes increasingly similar with burning

Results from our study highlighted DOM was unique across land cover types but became increasingly similar with increased burn severity. The enriched protein-like fluorescence signals and aliphatic N (e.g., peptide-like) containing signatures in the unburned forest leachates were depleted at high severities in favor of more red-shifted fluorescence, aromatic (e.g., increased $SUVA_{254}$, AImod, condensed aromatics), and aromatic N containing signatures. The overall increasing aromaticity and red-shifting fluorescence may in part be explained by the loss of lignin-like moieties, which are abundant in woody materials and undergo polymerization to more complex poly-aromatic structures when burned (Bird et al., 2015; Y. Chen et al., 2022). Similarly, with burning, proteins and other N-containing compounds can be taken up into more complex 5- and 6-membered aromatic structures, otherwise termed pyrogenic organic nitrogen (Torres-Rojas et al., 2020; Wagner et al., 2015a). This likely led to the proportionally higher intensity weighted N signature observed for forest leachates in this study as CHO containing components (cellulose/lignocellulose) are preferentially mineralized and N is taken up into the aromatic fraction of the bulk organic matter pool (Knicker, 2010).

The response of shrubland land cover types was distinct but more muted compared to that of the forest land cover types. The slight blue-shifting of fluorescence signals in addition to only slight molecular changes in aromatic signals (not condensed aromatic) indicate a shift to more structurally simple DOM at higher severities. Structurally complex plant materials have been linked with losses in molecular functionality with burning, which we suspect may disrupt intramolecular interactions that have been linked to long wavelength fluorescence signatures (Chebykina and Abakumov, 2022; Del Vecchio et al., 2017). Additionally, field studies have also indicated minimal production of condensed aromatic compounds in shrubland fires, however, there may still be increased overall aromaticity due to transformation of cellulose components (Alexis et al., 2010). This result would indicate that shrubland generated DOM formed from fire activity represents a smaller group of aromatic clusters rather than a proportionately higher presence of condensed aromatic compounds.

Similar to the forest land cover types, we again observed shifts for the shrubland land cover types in average molecular N signature, although this shift was driven predominantly by an increase in peptide-like signals (Fig. 4). This result was surprising as we would have expected burning to remove peptide-like signals through conversion to more aromatic-N functionality (Knicker, 2010). However, the release of proteins has been also previously reported in leachates of low temperature (<300 °C) chars (Zhang et al., 2023). As shrubland fires are typically rapid and do not often burn at equivalently high severities to that of forested systems (Stavi, 2019), we suspect the increasing protein-like formula for this land cover type may be the result of a breakdown in cellular structures that allow for the release of more labile DOM components. Such a mechanism has validity for other disturbance regimes, such as droughts or freeze thaw cycling (Halverson et al., 2000; Skogland et al., 1988); however, to our knowledge it has yet to be considered as a mechanism of release from low severity wildfires.

Despite some notable differences in molecular level chemistry across the land cover types, select bulk-scale optical signatures are indicative of broad aromaticity convergent with increasing burn severity. Such a convergence is consistent with current paradigms centered around the 'molecular thermometer' where high combustion temperatures generate less soluble but more aromatic DOC (Bostick et al., 2018; Schneider et al., 2013; Wagner et al., 2018; Zhang et al., 2023). However, aromaticity indicators, such as $SUVA_{254}$, were poorly linked with

maximum charring temperature (Section 3.1), an observation likely driven by the heterogeneity in our open air experimental design that created a realistic mosaic of burn severities across a range of burn conditions not exclusively reliant on temperature (Myers-Pigg et al., 2024a). Similarly, all land cover types converged to a common fluorescence signature consisting primarily of components C2 and C3 (UV-A and common M-peaks) at high severities (Fig. 3). Other field- and laboratory- based studies have also reported a linkage between the M peak and fire activity (Fischer et al., 2023; Zhang et al., 2023), indicating potential use of select fluorescence signatures in identifying short-term wildfire impacts in aquatic networks. Our study, though, highlights the shifts in DOM composition across land cover types that generate compositionally similar optical signatures with increasing burn severity.

5. Conclusions

Our results highlight the importance of land cover type in describing the molecular changes in DOM leached from chars along a gradient of burn severity. In general, across the forested and shrubland land cover types, DOM compositional changes trended toward increasing N and aromatic content. The extent of this aromatization was greater in the forest land cover types, which we suspect was due to a macromolecular makeup (e.g., lignin) that was more favorable for conversion to highly condensed aromatic compounds. These generalizable trends were reasonably anticipated based on previous temperature-based studies, although we did not observe direct linkages with maximum charring temperature. This disconnect was likely due to the high ecosystem-level variation and burn conditions we considered in our study, highlighting the importance of considering burn severity more directly as a broad indicator of post-wildfire ecosystem disturbance in biogeochemical studies.

Our results also provided first steps at developing a conceptual framework of DOM changes along burn severity gradients for major land cover types of the PNW (Fig. 5). Such frameworks may be more directly relatable to field based observations, as observed in a recent PNW wildfire study where high catchment burn severity was directly linked with storm flushing of aromatic N signatures in small streams (Roebuck et al., 2022). Additionally, scientists using reactive transport and other hydrological modeling are keen to integrate molecular level dynamics across burn severity gradients for describing disturbance-based impacts on river ecosystem function (Muller et al., 2024). Such efforts may in part be used to better describe the heterogeneous role of wildfire impacted DOM in microbially mediated processes (e.g., metabolism) (Graham et al., 2023) and transport along fluvial networks to coastal regions. We recognize the continued need to better integrate other environmental components, such as burned soils, into these conceptual frameworks linking DOM composition with burn severity (Fernández and Vega, 2016; Vega et al., 2013). Hydrologic transport through soils represents a key mechanism for DOM export where shifts in flowpaths throughout burned surface layers will directly impact composition of mobilized DOM. Such pathways may vary considerably between forest and shrubland land cover types where climate and antecedent water availability impact surface and subsurface water movement and lateral DOC exports to streams. Continuing to increase our understanding of DOM transformations along burn severity gradients will increase our ability to better predict wildfire disturbance impacts to terrestrial and aquatic biogeochemical cycles.

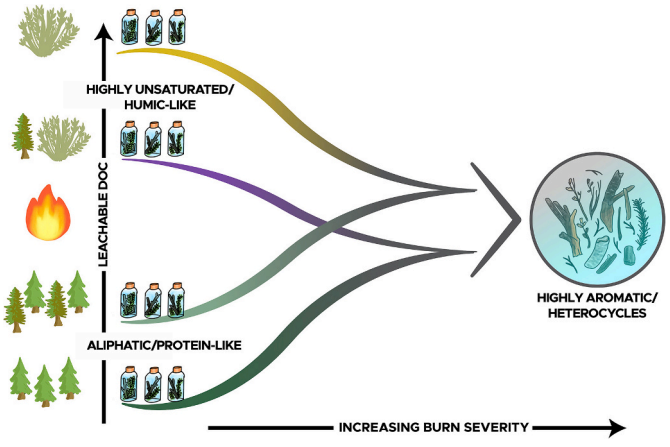

Fig. 5. Conceptual diagram molecular level changes in the chemical composition of DOM from across the PNW land cover categories with increasing burn severity.

CRediT authorship contribution statement

J. Alan Roebuck Jr: Writing – review & editing, Writing – original draft, Visualization, Validation, Software, Methodology, Investigation, Formal analysis, Data curation, Conceptualization. **Samantha Grieger:** Writing – review & editing, Writing – original draft, Validation, Software, Methodology, Investigation, Conceptualization. **Morgan E. Barnes:** Writing – review & editing, Writing – original draft, Visualization, Validation, Software, Methodology, Investigation, Formal analysis, Conceptualization. **Xia Gillespie:** Writing – review & editing, Writing – original draft, Visualization. **Kevin D. Bladon:** Writing – review & editing, Resources, Methodology, Conceptualization. **John D. Bailey:** Writing – review & editing, Resources, Methodology. **Emily B. Graham:** Writing – review & editing, Methodology, Conceptualization. **Rosalie Chu:** Writing – review & editing, Validation, Investigation. **William Kew:** Writing – review & editing, Validation, Investigation. **Timothy D. Scheibe:** Writing – review & editing, Resources, Funding acquisition, Conceptualization. **Allison N. Myers-Pigg:** Writing – review & editing, Writing – original draft, Validation, Supervision, Software, Resources, Project administration, Methodology, Funding acquisition, Formal analysis, Data curation, Conceptualization.

Declaration of competing interest

The authors declare that they have no known competing financial interests or personal relationships that could have appeared to influence the work reported in this paper.

Acknowledgments

This research was supported by the U.S. Department of Energy, Office of Science, Office of Biological and Environmental Research, Environmental System Science (ESS) Program. This contribution originates from the River Corridor Scientific Focus Area (SFA) project at Pacific Northwest National Laboratory (PNNL). A portion of this research was performed at the Environmental Molecular Sciences Laboratory (EMSL) User Facility. Pacific Northwest National Laboratory is operated by Battelle Memorial Institute for the U. S. Department of Energy under Contract DE-AC05-76RL01830.

Appendix A. Supplementary data

Supplementary data to this article can be found online at https://doi.org/10.1016/j.scitotenv.2024.178040.

Data availability

A comprehensive assessment for this open air burn experiment, including relevant metadata information on vegetation collection and treatments, burn protocols and workflows, photos, and videos is publicly available on the Environmental System Science Data Infrastructure for a Virtual Ecosystem (ESS-DIVE) data repository (Grieger et al., 2022). Dissolved organic carbon, absorbance scans, Raman normalized 3D

excitation-emission fluorescence scans, FTICR-MS instrument files, and FTICR-MS processing instructions are also available at Grieger et al. (2022). Additional data (including PARAFAC results and processed FTICR-MS data) and scripts needed to reproduce statistics and figures for this manuscript are available at Myers-Pigg et al. (2024b).

References

Alexis, M.A., Rumpel, C., Knicker, H., Leifeld, J., Rasse, D., Péchot, N., Bardoux, G., Mariotti, A., 2010. Thermal alteration of organic matter during a shrubland fire: a field study. Org. Geochem. 41, 690–697. https://doi.org/10.1016/j.orggeochem.2010.03.003.

Bates, D., Mächler, M., Bolker, B., Walker, S., 2015. Fitting linear mixed-effects models using lme4. J. Stat. Softw. 67, 1–48. https://doi.org/10.18637/jss.v067.i01.

Bird, M.I., Wynn, J.G., Saiz, G., Wurster, C.M., McBeath, A., 2015. The pyrogenic carbon cycle. Annu. Rev. Earth Planet. Sci. 43, 273–298. https://doi.org/10.1146/annurev-earth-060614-105038.

Bladon, K.D., Emelko, M.B., Silins, U., Stone, M., 2014. Wildfire and the future of water supply. Environ. Sci. Technol. 48, 8936–8943. https://doi.org/10.1021/es500130g.

Bodí, M.B., Martin, D.A., Balfour, V.N., Santín, C., Doerr, S.H., Pereira, P., Cerdà, A., Mataix-Solera, J., 2014. Wildland fire ash: production, composition and eco-hydro-geomorphic effects. Earth Sci. Rev. 130, 103–127. https://doi.org/10.1016/j.earscirev.2013.12.007.

Boot, C.M., Haddix, M., Paustian, K., Cotrufo, M.F., 2014. Distribution of black carbon in Ponderosa pine litter and soils following the High Park wildfire. Biogeosci. Discuss. 11, 16799–16824. https://doi.org/10.5194/bgd-11-16799-2014.

Bostick, K.W., Zimmerman, A.R., Wozniak, A.S., Mitra, S., Hatcher, P.G., 2018. Production and composition of pyrogenic dissolved organic matter from a logical series of laboratory-generated chars. Front. Earth Sci. China 6. https://doi.org/10.3389/feart.2018.00043.

Bostick, K.W., Zimmerman, A.R., Goranov, A.I., Mitra, S., Hatcher, P.G., Wozniak, A.S., 2020. Photolability of pyrogenic dissolved organic matter from a thermal series of laboratory-prepared chars. Sci. Total Environ. 724, 138198. https://doi.org/10.1016/j.scitotenv.2020.138198.

Bowman, D.M.J.S., Balch, J.K., Artaxo, P., Bond, W.J., Carlson, J.M., Cochrane, M.A., D'Antonio, C.M., Defries, R.S., Doyle, J.C., Harrison, S.P., Johnston, F.H., Keeley, J. E., Krawchuk, M.A., Kull, C.A., Marston, J.B., Moritz, M.A., Prentice, I.C., Roos, C.I., Scott, A.C., Swetnam, T.W., van der Werf, G.R., Pyne, S.J., 2009. Fire in the Earth system. Science 324, 481–484. https://doi.org/10.1126/science.1163886.

Brucker, C.P., Livneh, B., Minear, J.T., Rosario-Ortiz, F.L., 2022. A review of simulation experiment techniques used to analyze wildfire effects on water quality and supply. Environ Sci Process Impacts 24, 1110–1132. https://doi.org/10.1039/d2em00045h.

Cao, X., Li, S.-A., Huang, H., Ma, H., 2024. Wildfire impacts on molecular changes of dissolved organic matter during its passage through soil. Environ. Sci. Technol. 58, 11436–11446. https://doi.org/10.1021/acs.est.3c11056.

Cawley, K.M., Hohner, A.K., Podgorski, D.C., Cooper, W.T., Korak, J.A., Rosario-Ortiz, F. L., 2017. Molecular and spectroscopic characterization of water extractable organic matter from thermally altered soils reveal insight into disinfection byproduct precursors. Environ. Sci. Technol. 51, 771–779. https://doi.org/10.1021/acs.est.6b05126.

Chebykina, E., Abakumov, E., 2022. Essential role of forest fires in humic acids structure and composition alteration. Agronomy 12, 2910. https://doi.org/10.3390/agronomy12122910.

Chen, Y., Sun, K., Sun, H., Yang, Y., Li, Y., Gao, B., Xing, B., 2022a. Photodegradation of pyrogenic dissolved organic matter increases bioavailability: novel insight into bioalteration, microbial community succession, and C and N dynamics. Chem. Geol. 605, 120964. https://doi.org/10.1016/j.chemgeo.2022.120964.

Chen, H., Wang, J., Zhao, X., Wang, Y., Huang, Z., Gong, T., Xian, Q., 2022b. Occurrence of dissolved black carbon in source water and disinfection byproducts formation during chlorination. J. Hazard. Mater. 435, 129054. https://doi.org/10.1016/j.jhazmat.2022.129054.

Coble, P.G., 1996. Characterization of marine and terrestrial DOM in seawater using excitation-emission matrix spectroscopy. Mar. Chem. 51, 325–346. https://doi.org/10.1016/0304-4203(95)00062-3.

Cook, W.C., Harris, L.E., 1968. Bulletin No. 472 - Nutritive Value of Seasonal Ranges. UAES Bulletins. UAES Bulletins.

Coppola, A.I., Druffel, E.R.M., 2016. Cycling of black carbon in the ocean. Geophys. Res. Lett. https://doi.org/10.1002/2016GL068574.

Coppola, A.I., Wagner, S., Lennartz, S.T., Seidel, M., Ward, N.D., Dittmar, T., Santín, C., Jones, M.W., 2022. The black carbon cycle and its role in the Earth system. Nature Reviews Earth & Environment 3, 516–532. https://doi.org/10.1038/s43017-022-00316-6.

Dahm, C.N., Candelaria-Ley, R.I., Reale, C.S., Reale, J.K., Van Horn, D.J., 2015. Extreme water quality degradation following a catastrophic forest fire. Freshw. Biol. 60, 2584–2599. https://doi.org/10.1111/fwb.12548.

de la Rosa, J.M., Knicker, H., 2011. Bioavailability of N released from N-rich pyrogenic organic matter: an incubation study. Soil Biol. Biochem. 43, 2368–2373. https://doi.org/10.1016/j.soilbio.2011.08.008.

Del Vecchio, R., Schendorf, T.M., Blough, N.V., 2017. Contribution of quinones and ketones/aldehydes to the optical properties of humic substances (HS) and chromophoric dissolved organic matter (CDOM). Environ. Sci. Technol. 51, 13624–13632. https://doi.org/10.1021/acs.est.7b04172.

Dittmar, T., de Rezende, C.E., Manecki, M., Niggemann, J., Coelho Ovalle, A.R., Stubbins, A., Bernardes, M.C., 2012. Continuous flux of dissolved black carbon from a vanished tropical forest biome. Nat. Geosci. 5, 618–622. https://doi.org/10.1038/ngeo1541.

Fengel, D., Wegener, G., 2011. Wood: Chemistry, Ultrastructure, Reactions. Walter de Gruyter. https://doi.org/10.1515/9783110839654.

Fernández, C., Vega, J.A., 2016. Modelling the effect of soil burn severity on soil erosion at hillslope scale in the first year following wildfire in NW Spain. Earth Surf. Process. Landf. 41, 928–935. https://doi.org/10.1002/esp.3876.

Fischer, S.J., Fegel, T.S., Wilkerson, P.J., Rivera, L., Rhoades, C.C., Rosario-Ortiz, F.L., 2023. Fluorescence and absorbance indices for dissolved organic matter from wildfire ash and burned watersheds. ACS EST Water 3, 2199–2209. https://doi.org/10.1021/acsestwater.3c00017.

Francis, E.J., Pourmohammadi, P., Steel, Z.L., Collins, B.M., Hurteau, M.D., 2023. Proportion of forest area burned at high-severity increases with increasing forest cover and connectivity in western US watersheds. Landsc. Ecol. 38, 2501–2518. https://doi.org/10.1007/s10980-023-01710-1.

Graham, E.B., Song, H.-S., Grieger, S., Garayburu-Caruso, V.A., Stegen, J.C., Bladon, K. D., Myers-Pigg, A.N., 2023. Potential bioavailability of representative pyrogenic organic matter compounds in comparison to natural dissolved organic matter pools. Biogeosciences 20, 3449–3457. https://doi.org/10.5194/bg-20-3449-2023.

Grieger, S., Aronstein, P., Bailey, J., Barnes, M., Barton, R., Bladon, K.D., Chu, R., Forbes, B., Garayburu-Caruso, V.A., Graham, E.B., Goldman, A.E., Homolka, K., Kew, W., Lipton, A.S., McKever, S.A., Munson, K.M., Myers, C.R., Nieto-Pereira, N., O'Day, P., Otenburg, O., Renteria, L., Roebuck, A., Scheibe, T.D., Torgeson, J.M., Toyoda, J.G., Wagner, S., Young, R.P., Myers-Pigg, A., 2022. Organic Matter Concentration and Composition of Experimentally Burned Open Air and Muffle Furnace Vegetation Chars Across Differing Burn Severity and Feedstock Types From Pacific Northwest, USA (v3). https://doi.org/10.15485/1894135.

Halofsky, J.E., Peterson, D.L., Harvey, B.J., 2020. Changing wildfire, changing forests: the effects of climate change on fire regimes and vegetation in the Pacific Northwest, USA. Fire Ecol. 16, 4. https://doi.org/10.1186/s42408-019-0062-8.

Halverson, L.J., Jones, T.M., Firestone, M.K., 2000. Release of intracellular solutes by four soil bacteria exposed to dilution stress. Soil Sci. Soc. Am. J. 64, 1630–1637. https://doi.org/10.2136/sssaj2000.6451630x.

Hansen, A.M., Kraus, T.E.C., Pellerin, B.A., Fleck, J.A., Downing, B.D., Bergamaschi, B.A., 2016. Optical properties of dissolved organic matter (DOM): effects of biological and photolytic degradation. Limnol. Oceanogr. 61, 1015–1032. https://doi.org/10.1002/lno.10270.

Hudiburg, T., Mathias, J., Bartowitz, K., Berardi, D.M., Bryant, K., Graham, E., Kolden, C. A., Betts, R.A., Lynch, L., 2023. Terrestrial carbon dynamics in an era of increasing wildfire. Nat. Clim. Chang. 13, 1306–1316. https://doi.org/10.1038/s41558-023-01881-4.

Jaffé, R., Ding, Y., Niggemann, J., Vähätalo, A.V., Stubbins, A., Spencer, R.G.M., Campbell, J., Dittmar, T., 2013. Global charcoal mobilization from soils via dissolution and riverine transport to the oceans. Science 340, 345–347. https://doi.org/10.1126/science.1231476.

Johnston, S.G., Maher, D.T., 2022. Drought, megafires and flood - climate extreme impacts on catchment-scale river water quality on Australia's east coast. Water Res. 218, 118510. https://doi.org/10.1016/j.watres.2022.118510.

Keeley, J.E., 2009. Fire intensity, fire severity and burn severity: a brief review and suggested usage. Int. J. Wildland Fire 18, 116–126. https://doi.org/10.1071/WF07049.

Knicker, H., 2010. "Black nitrogen" – an important fraction in determining the recalcitrance of charcoal. Org. Geochem. 41, 947–950. https://doi.org/10.1016/j.orggeochem.2010.04.007.

Koch, B.P., Dittmar, T., 2006. From mass to structure: an aromaticity index for high-resolution mass data of natural organic matter. Rapid Commun. Mass Spectrom. 20, 926–932. https://doi.org/10.1002/rcm.2386.

Koch, B.P., Dittmar, T., 2016. From mass to structure: an aromaticity index for high-resolution mass data of natural organic matter. Rapid Commun. Mass Spectrom. 30, 250. https://doi.org/10.1002/rcm.7433.

Kufeld, R.C., Stevens, M., Bowden, D.C., 1981. Winter variation in nutrient and fiber content and in vitro digestibility of gambel oak (Quercus gambellii) and big sagebrush (Artemisia tridentata) from diversified sites in Colorado. J. Range Manage. 34, 149–151. https://doi.org/10.2307/3898133.

LaRowe, D.E., Van Cappellen, P., 2011. Degradation of natural organic matter: a thermodynamic analysis. Geochim. Cosmochim. Acta 75, 2030–2042. https://doi.org/10.1016/j.gca.2011.01.020.

Lenth, R., 2023. emmeans: Estimated Marginal Means, aka Leas-Squares Means.

Li, M., Zhang, A., Wu, H., Liu, H., Lv, J., 2017. Predicting potential release of dissolved organic matter from biochars derived from agricultural residues using fluorescence and ultraviolet absorbance. J. Hazard. Mater. 334, 86–92. https://doi.org/10.1016/j.jhazmat.2017.03.064.

Li, Zhi, Li, B., Jiang, P., Hammond, G.E., Shuai, P., Coon, E., Chen, X., 2023a. Evaluating the Effects of Burn Severity and Precipitation on Post-Fire Watershed Responses Using Distributed Hydrologic Models. https://doi.org/10.22541/essoar.170224575.51711472/v1.

Li, Zhao, Samonte, P.R.V., Cao, H., Miesel, J.R., Xu, W., 2023b. Assess the formation of disinfection by-products from pyrogenic dissolved organic matter (pyDOM): impact of wildfire on the water quality of forest watershed. Sci. Total Environ. 898, 165496. https://doi.org/10.1016/j.scitotenv.2023.165496.

Littell, J.S., Oneil, E.E., McKenzie, D., Hicke, J.A., Lutz, J.A., Norheim, R.A., Elsner, M. M., 2010. Forest ecosystems, disturbance, and climatic change in Washington State, USA. Clim. Change 102, 129–158. https://doi.org/10.1007/s10584-010-9858-x.

Liu, P., Ptacek, C.J., Blowes, D.W., Berti, W.R., Landis, R.C., 2015. Aqueous leaching of organic acids and dissolved organic carbon from various biochars prepared at

different temperatures. J. Environ. Qual. 44, 684–695. https://doi.org/10.2134/jeq2014.08.0341.
Luo, Y., Durenkamp, M., De Nobili, M., Lin, Q., Brookes, P.C., 2011. Short term soil priming effects and the mineralisation of biochar following its incorporation to soils of different pH. Soil Biol. Biochem. 43, 2304–2314. https://doi.org/10.1016/j.soilbio.2011.07.020.
Marlon, J.R., Bartlein, P.J., Gavin, D.G., Long, C.J., Anderson, R.S., Briles, C.E., Brown, K. J., Colombaroli, D., Hallett, D.J., Power, M.J., Scharf, E.A., Walsh, M.K., 2012. Long-term perspective on wildfires in the western USA. Proc. Natl. Acad. Sci. U. S. A. 109, E535–E543. https://doi.org/10.1073/pnas.1112839109.
Masiello, C.A., 2004. New directions in black carbon organic geochemistry. Mar. Chem. 92, 201–213. https://doi.org/10.1016/j.marchem.2004.06.043.
McKay, G., Hohner, A.K., Rosario-Ortiz, F.L., 2020. Use of optical properties for evaluating the presence of pyrogenic organic matter in thermally altered soil leachates. Environ Sci Process Impacts 22, 981–992. https://doi.org/10.1039/c9em00413k.
Mukherjee, A., Zimmerman, A.R., 2013. Organic carbon and nutrient release from a range of laboratory-produced biochars and biochar–soil mixtures. Geoderma 193–194, 122–130. https://doi.org/10.1016/j.geoderma.2012.10.002.
Muller, K.A., Jiang, P., Hammond, G., 2024. Lambda-PFLOTRAN 1.0: Workflow for Incorporating Organic Matter Chemistry Informed by Ultra High Resolution Mass Spectrometry Into Biogeochemical Modeling. Geoscientific Model. https://doi.org/10.5194/gmd-2024-34.
Murphy, K.R., Stedmon, C.A., Graeber, D., Bro, R., 2013. Fluorescence spectroscopy and multi-way techniques. PARAFAC. Anal. Methods 5, 6557–6566. https://doi.org/10.1039/C3AY41160E.
Myers-Pigg, A.N., Louchouarn, P., Teisserenc, R., 2017. Flux of dissolved and particulate low-temperature pyrogenic carbon from two high-latitude rivers across the spring freshet hydrograph. Front. Mar. Sci. 4. https://doi.org/10.3389/fmars.2017.00038.
Myers-Pigg, A.N., Grieger, S., Roebuck Jr., J.A., Barnes, M.E., Bladon, K.D., Bailey, J.D., Barton, R., Chu, R.K., Graham, E.B., Homolka, K.K., Kew, W., Lipton, A.S., Scheibe, T., Toyoda, J.G., Wagner, S., 2024a. Experimental open air burning of vegetation enhances organic matter chemical heterogeneity compared to laboratory burns. Environ. Sci. Technol. 58, 9679–9688. https://doi.org/10.1021/acs.est.3c10826.
Myers-Pigg, A.N., Roebuck, A., Forbes, B., Powers-McCormack, B., 2024b. Manuscript Workflows From and Processed Organic Matter Composition of Experimentally Burned Open Air and Muffle Furnace Vegetation Chars Across Differing Burn Severity and Feedstock Types From Pacific Northwest, USA. https://doi.org/10.15485/2327028.
Norwood, M.J., Louchouarn, P., Kuo, L.J., Harvey, O.R., 2013. Characterization and biodegradation of water-soluble biomarkers and organic carbon extracted from low temperature chars. Org. Geochem. 56, 111–119.
Ohno, T., 2002. Fluorescence inner-filtering correction for determining the humification index of dissolved organic matter. Environ. Sci. Technol. 36, 742–746. https://doi.org/10.1021/es0155276.
Olivares, C.I., Zhang, W., Uzun, H., Erdem, C.U., Majidzadeh, H., Trettin, C., Karanfil, T., Chow, A., 2019. Optical in-situ sensors capture dissolved organic carbon (DOC) dynamics after prescribed fire in high-DOC forest watersheds. Int. J. Wildland Fire 28, 761–768. https://doi.org/10.1071/WF18175.
Parsons, A., Robichaud, P.R., Lewis, S.A., Napper, C., 2010. Field Guide for Mapping Post-Fire Soil Burn Severity. Citeseer.
Patel, K.F., 2020. kaizadp/fticrrr: FTICR-Results-in-R. https://doi.org/10.5281/zenodo.3893246.
R Core Team, 2023. R: A Language and Environment for Statistical Computing. R Foundation for Statistical Computing, Vienna, Austria.
Rahman, Mohammed Mahabubur, Tsukamoto, J., Rahman, Md Motiur, Yoneyama, A., Mostafa, K.M., 2013. Lignin and its effects on litter decomposition in forest ecosystems. Chem. Ecol. 29, 540–553. https://doi.org/10.1080/02757540.2013.790380.
Rajapaksha, A.U., Ok, Y.S., El-Naggar, A., Kim, H., Song, F., Kang, S., Tsang, Y.F., 2019. Dissolved organic matter characterization of biochars produced from different feedstock materials. J. Environ. Manage. 233, 393–399. https://doi.org/10.1016/j.jenvman.2018.12.069.
Reilly, M.J., Dunn, C.J., Meigs, G.W., Spies, T.A., 2017. Contemporary patterns of fire extent and severity in forests of the Pacific Northwest, USA (1985–2010). Ecosphere. https://doi.org/10.1002/ecs2.1695.
Roebuck Jr., J.A., Bladon, K.D., Donahue, D., Graham, E.B., Grieger, S., Morgenstern, K., Norwood, M.J., Wampler, K.A., Erkert, L., Renteria, L., Danczak, R., Fricke, S., Myers-Pigg, A.N., 2022. Spatiotemporal controls on the delivery of dissolved organic matter to streams following a wildfire. Geophys. Res. Lett. 49 (16), e2022GL099535.
Roebuck Jr., J.A., Medeiros, P.M., Letourneau, M.L., Jaffé, R., 2018a. Hydrological controls on the seasonal variability of dissolved and particulate black carbon in the Altamaha River, GA. J. Geophys. Res. Biogeosci. 123, 3055–3071. https://doi.org/10.1029/2018jg004406.
Roebuck Jr., J.A., Seidel, M., Dittmar, T., Jaffé, R., 2018b. Land use controls on the spatial variability of dissolved black carbon in a subtropical watershed. Environ. Sci. Technol. 52, 8104–8114. https://doi.org/10.1021/acs.est.8b00190.
Roth, H.K., Borch, T., Young, R.B., Bahureksa, W., Blakney, G.T., Nelson, A.R., Wilkins, M.J., McKenna, A.M., 2022. Enhanced speciation of pyrogenic organic matter from wildfires enabled by 21 T FT-ICR mass spectrometry. Anal. Chem. 94, 2973–2980. https://doi.org/10.1021/acs.analchem.1c05018.
Rust, A.J., Saxe, S., McCray, J., Rhoades, C.C., Hogue, T.S., 2019. Evaluating the factors responsible for post-fire water quality response in forests of the western USA. Int. J. Wildland Fire 28, 769–784. https://doi.org/10.1071/WF18191.
Santín, C., Doerr, S.H., Preston, C.M., González-Rodríguez, G., 2015. Pyrogenic organic matter production from wildfires: a missing sink in the global carbon cycle. Glob. Chang. Biol. 21, 1621–1633. https://doi.org/10.1111/gcb.12800.
Santín, C., Doerr, S.H., Kane, E.S., Masiello, C.A., Ohlson, M., de la Rosa, J.M., Preston, C. M., Dittmar, T., 2016. Towards a global assessment of pyrogenic carbon from vegetation fires. Glob. Chang. Biol. 22, 76–91. https://doi.org/10.1111/gcb.12985.
Schneider, M.P.W., Pyle, L.A., Clark, K.L., Hockaday, W.C., Masiello, C.A., Schmidt, M.W. I., 2013. Toward a "molecular thermometer" to estimate the charring temperature of wildland charcoals derived from different biomass sources. Environ. Sci. Technol. 47, 11490–11495. https://doi.org/10.1021/es401430f.
Seidel, M., Yager, P.L., Ward, N.D., Carpenter, E.J., Gomes, H.R., Krusche, A.V., Richey, J.E., Dittmar, T., Medeiros, P.M., 2015. Molecular-level changes of dissolved organic matter along the Amazon River-to-ocean continuum. Mar. Chem. 177, 218–231. https://doi.org/10.1016/j.marchem.2015.06.019.
Serafim, T.S.G, de Almeida, M.G., Thouzeau, G., Michaud, E., Niggemann, J., Dittmar, T., Seidel, M., de Rezende, C.E., 2023. Land-use changes in Amazon and Atlantic rainforests modify organic matter and black carbon compositions transported from land to the coastal ocean. Sci. Total Environ. 878, 162917. https://doi.org/10.1016/j.scitotenv.2023.162917.
Shakesby, R.A., Bento, C.P.M., Ferreira, C.S.S., Ferreira, A.J.D., Stoof, C.R., Urbanek, E., Walsh, R.P.D., 2015. Impacts of prescribed fire on soil loss and soil quality: an assessment based on an experimentally-burned catchment in central Portugal. Catena 128, 278–293. https://doi.org/10.1016/j.catena.2013.03.012.
Shaw, J.B., Lin, T.-Y., Leach 3rd, F.E., Tolmachev, A.V., Tolić, N., Robinson, E.W., Koppenaal, D.W., Paša-Tolić, L., 2016. 21 Tesla Fourier transform ion cyclotron resonance mass spectrometer greatly expands mass spectrometry toolbox. J. Am. Soc. Mass Spectrom. 27, 1929–1936. https://doi.org/10.1007/s13361-016-1507-9.
Skogland, T., Lomeland, S., Goksøyr, J., 1988. Respiratory burst after freezing and thawing of soil: experiments with soil bacteria. Soil Biol. Biochem. 20, 851–856. https://doi.org/10.1016/0038-0717(88)90092-2.
Stavi, I., 2019. Wildfires in grasslands and shrublands: a review of impacts on vegetation, soil, hydrology, and geomorphology. Water 11, 1042. https://doi.org/10.3390/w11051042.
Stedmon, C.A., Markager, S., Bro, R., 2003. Tracing dissolved organic matter in aquatic environments using a new approach to fluorescence spectroscopy. Mar. Chem. 82, 239–254. https://doi.org/10.1016/S0304-4203(03)00072-0.
Thuile Bistarelli, L., Poyntner, C., Santín, C., Doerr, S.H., Talluto, M.V., Singer, G., Sigmund, G., 2021. Wildfire-derived pyrogenic carbon modulates riverine organic matter and biofilm enzyme activities in an in situ flume experiment. ACS ES T Water 1, 1648–1656. https://doi.org/10.1021/acsestwater.1c00185.
Tolić, N., Liu, Y., Liyu, A., Shen, Y., Tfaily, M.M., Kujawinski, E.B., Longnecker, K., Kuo, L.-J., Robinson, E.W., Paša-Tolić, L., Hess, N.J., 2017. Formularity: software for automated formula assignment of natural and other organic matter from ultrahigh-resolution mass spectra. Anal. Chem. 89, 12659–12665. https://doi.org/10.1021/acs.analchem.7b03318.
Torres-Rojas, D., Hestrin, R., Solomon, D., Gillespie, A.W., Dynes, J.J., Regier, T.Z., Lehmann, J., 2020. Nitrogen speciation and transformations in fire-derived organic matter. Geochim. Cosmochim. Acta 276, 170–185. https://doi.org/10.1016/j.gca.2020.02.034.
Vega, J.A., Fontúrbel, T., Merino, A., Fernández, C., Ferreiro, A., Jiménez, E., 2013. Testing the ability of visual indicators of soil burn severity to reflect changes in soil chemical and microbial properties in pine forests and shrubland. Plant and Soil 369, 73–91. https://doi.org/10.1007/s11104-012-1532-9.
Wagner, S., Dittmar, T., Jaffé, R., 2015a. Molecular characterization of dissolved black nitrogen via electrospray ionization Fourier transform ion cyclotron resonance mass spectrometry. Org. Geochem. 79, 21–30. https://doi.org/10.1016/j.orggeochem.2014.12.002.
Wagner, S., Riedel, T., Niggemann, J., Vähätalo, A.V., Dittmar, T., Jaffé, R., 2015b. Linking the molecular signature of heteroatomic dissolved organic matter to watershed characteristics in world rivers. Environ. Sci. Technol. 49, 13798–13806. https://doi.org/10.1021/acs.est.5b00525.
Wagner, S., Jaffé, R., Stubbins, A., 2018. Dissolved black carbon in aquatic ecosystems. Limnol. Oceanogr. Lett. 3, 168–185. https://doi.org/10.1002/lol2.10076.
Wampler, K.A., Bladon, K.D., Faramarzi, M., 2023. Modeling wildfire effects on streamflow in the Cascade Mountains, Oregon, USA. J. Hydrol. https://doi.org/10.1016/j.jhydrol.2023.129585.
Welch, B.L., 1997. Comment: big sagebrush pro versus con. J. Range Manage. 50, 322. https://doi.org/10.2307/4003736.
Wheeler, K.I., Levia, D.F., Hudson, J.E., 2017. Tracking senescence-induced patterns in leaf litter leachate using parallel factor analysis (PARAFAC) modeling and self-organizing maps. Eur. J. Vasc. Endovasc. Surg. 122, 2233–2250. https://doi.org/10.1002/2016jg003677.
White, H., 1980. A heteroskedasticity-consistent covariance matrix estimator and a direct test for heteroskedasticity. Econometrica 48, 817–838. https://doi.org/10.2307/1912934.

Wilkerson, P.J., Rosario-Ortiz, F.L., 2021. Impact of simulated wildfire on disinfection byproduct formation potential. AWWA Water Sci. 3. https://doi.org/10.1002/aws2.1217.

Wozniak, A.S., Goranov, A.I., Mitra, S., Bostick, K.W., Zimmerman, A.R., Schlesinger, D. R., Myneni, S., Hatcher, P.G., 2020. Molecular heterogeneity in pyrogenic dissolved organic matter from a thermal series of oak and grass chars. Org. Geochem. 148, 104065. https://doi.org/10.1016/j.orggeochem.2020.104065.

Wünsch, U.J., Bro, R., Stedmon, C.A., Wenig, P., Murphy, K.R., 2019. Emerging patterns in the global distribution of dissolved organic matter fluorescence. Anal. Methods 11, 888–893. https://doi.org/10.1039/C8AY02422G.

Yin, G., Guan, P., Wang, Y.-H., Zhang, P., Qu, B., Xu, S., Zhang, G., He, C., Shi, Q., Wang, J., 2024. Temporal variations in fire impacts on characteristics and composition of soil-derived dissolved organic matter at Qipan Mountain, China. Environ. Sci. Technol. 58, 13772–13782. https://doi.org/10.1021/acs.est.4c00446.

Zhang, Q., Wang, Y., Guan, P., Zhang, P., Mo, X., Yin, G., Qu, B., Xu, S., He, C., Shi, Q., Zhang, G., Dittmar, T., Wang, J., 2023. Temperature thresholds of pyrogenic dissolved organic matter in heating experiments simulating forest fires. Environ. Sci. Technol. 57, 17291–17301. https://doi.org/10.1021/acs.est.3c05265.

Zhu, S., Yang, P., Yin, Y., Zhang, S., Lv, J., Tian, S., Jiang, T., Wang, D., 2024. Influences of wildfire on the soil dissolved organic matter characteristics and its electron-donating capacity. Water Res. 266, 122382. https://doi.org/10.1016/j.watres.2024.122382.

Zimmerman, A.R., Mitra, S., 2017. Trial by fire: on the terminology and methods used in pyrogenic organic carbon research. Front. Earth Sci. China 5. https://doi.org/10.3389/feart.2017.00095.